Published in final edited form as:
J Immunol. 2013 November 1; 191(9): . doi:10.4049/jimmunol.1202673.

Neuraminidase reprograms lung tissue and potentiates LPS-induced acute lung injury in mice

Chiguang Feng[*], **Lei Zhang**[*], **Chinh Nguyen**[†], **Stefanie N. Vogel**[‡], **Simeon E. Goldblum**[†], **William C. Blackwelder**[*], and **Alan S. Cross**[*]

[*]Center for Vaccine Development, University of Maryland School of Medicine, Baltimore, Maryland, United States of America

[†]Mucosal Biology Research Center, University of Maryland School of Medicine, Baltimore, Maryland, United States of America

[‡]Department of Microbiology and Immunology, University of Maryland School of Medicine, Baltimore, Maryland, United States of America

Abstract

We previously reported that removal of sialyl residues primed PBMCs to respond to bacterial LPS stimulation *in vitro*. Therefore, we speculated that prior desialylation can sensitize the host to generate an enhanced inflammatory response upon exposure to a TLR ligand, such as LPS, in a murine model of acute lung injury. Intratracheal instillation of neuraminidase (NA) 30 min prior to intratracheal administration of LPS increased PMNs in the bronchoalveolar lavage fluid (BALF) and the wet-to-dry lung weight ratio, a measure of pulmonary edema, compared to mice that received LPS alone. Administration of NA alone resulted in desialylation of bronchiolar and alveolar surfaces and induction of TNF-α, IL-1β, and chemokines in lung homogenates and BALF; however, PMN recruitment in mice treated with NA alone did not differ from those of PBS-administered controls. NA pretreatment alone induced apoptosis and markedly enhanced LPS-induced endothelial apoptosis. Administration of recombinant Bcl-2, an anti-apoptotic molecule, abolished the effect of NA treatment on LPS-induced PMN recruitment and pulmonary edema formation. We conclude that NA pretreatment potentiates LPS-induced lung injury through enhanced PMN recruitment, pulmonary edema formation, and endothelial and myeloid cell apoptosis. A similar “reprogramming” of immune responses with desialylation may occur during respiratory infection with NA-expressing microbes and contribute to severe lung injury.

Introduction

Mammalian cell surfaces are covered with a broad range of carbohydrate structures, glycoproteins and glycolipids, that undergo considerable modification as the cells respond to physiologic and pathologic stimuli. These surface glycans are involved in cell-to-cell interactions and upon engagement with specific ligands (1-4), can initiate intracellular signaling cascades (5, 6). These events are critical to a wide range of biological processes including inflammation (7, 8). Further, glycotransferases and glycosidases, working in concert, regulate the fine structure and activity of these glycans (9, 10).

Sialic acids are widely distributed in animal tissues as gangliosides or glycoproteins on the cell surface (11). These highly negatively charged molecules are known to be important in T-B lymphocyte interactions, and act by masking antigens on host cell surfaces, regulating

Corresponding author: Alan S. Cross, M.D., Center for Vaccine Development, University of Maryland School of Medicine, 685 W. Baltimore Street, Baltimore, Maryland 21201; across@medicine.umaryland.edu; telephone: 410-706-5328; fax: 410-706-6206.

both receptor-ligand interactions and the life spans of proteins and cells that are cleared by asialoreceptors (11-14). Sialic acids also play a critical role in nerve cell development and in the metastatic potential of malignant cells (15, 16). Mammalian lung tissues are heavily sialylated with both α-2,6-linked and, to a lesser extent, α-2,3-linked sialic acids detected in alveoli (17, 18). Desialylation, or removal of terminal sialic acids, alters a wide range of cellular functions, including host cell responsiveness to bacterial stimulation (19-21). We have shown that desialylation increases LPS-induced ERK activation and cytokine expression in human PBMC (19). In TLR4-expressing HEK293 cells, we found that TLR4 and MD2 were sialylated, and their desialylation increased LPS-induced NF-κB activation (21). Stimulation of polymorphonuclear leukocytes (PMNs) both *in vitro* and *in vivo* enhanced PMN recruitment to inflamed sites via modulation of cell surface sialylation, presumably by promoting PMN adherence to and migration across the endothelium (22, 23). Inhibition of PMN sialidase activity either by pharmacologic inhibition or immune blockade diminished their recruitment to inflamed sites *in vivo* (23).

Microbial neuraminidases (NA), enzymes that cleave sialic acid from glycoconjugates in a glycosidic linkage-specific manner, are important virulence factors for pathogens, particularly those that target mucosal surfaces (24-26). For example, influenza virus NA is critical to its infective cycle and is therefore a target of antiviral therapy (24, 25). *Pseudomonas aeruginosa* and *Streptococcus pneumoniae* rely on NAs to colonize the mammalian host (26).

In human acute lung injury (ALI), neutrophilic alveolitis, deposition of hyaline membranes, and formation of microthrombi comprise three key pathological features (27). While murine models have been established for studying ALI, each displays only one or two characteristics of human ALI, but not all three. Intratracheal (i.t.) deposition of LPS induced intra-alveolar PMN infiltration (28).

We hypothesized that during respiratory infection with microbes that express NA, lung tissues may become desialylated. This may prime the host inflammatory response to a TLR ligand that may then exacerbate lung injury. To address this question, we adapted an LPS-induced ALI model with NA pre-treatment to study the effect of prior desialylation of mouse lung tissue in response to bacterial LPS stimulation *in vivo*. We now report that NA pretreatment sensitizes the host to LPS-induced PMN recruitment, proinflammatory cytokine production, apoptosis, and severe lung injury. Administration of exogenous recombinant human Bcl-2 (rhBcl-2), an anti-apoptotic molecule, partially reverses the lung injury. Our findings indicate that NA is a virulence factor that may potentiate the acute pro-inflammatory response to NA-expressing respiratory pathogens and exacerbate acute lung injury.

Materials and Methods

Animals

CD1 outbred mice were purchased from Charles River Laboratories, Inc. KC knockout mice ($KC^{-/-}$) on a C57BL/6 background were bred at UMB in the colony of Dr. Stefanie Vogel (29). C57BL/6 mice to serve as controls for $KC^{-/-}$ mice were purchased from Charles River Laboratories. All animals were maintained in the UMB animal facility under an approved IACUC protocol.

Reagents

C. perfringens NA (type X) and LPS (*E. coli* O111:B4) were purchased from Sigma. Biotinylated Peanut Agglutinin (PNA), Sambucus Nigra Lectin (SNA), and Maackia

Amurensis Lectin II (MAAII) were purchased from Vector Laboratories. Recombinant human Bcl-2 (rhBcl-2) was purchased from R&D Systems.

LPS-induced ALI

To induce ALI, 5 μg of LPS (25 μl at 0.2 mg/ml) in sterile PBS was administered into the tracheas of anesthetized animals as described (30). For NA treatment, 100 mU of NA (25 μl at 4 U/ml) in PBS was similarly deposited, 30 min before LPS challenge. This was the minimal dose required to desialylate lung tissue to an extent similar to that observed with experimental influenza infection (Nita-Lazar M, Pasek M, Chen W, Feng C, Cross A, Rabinovich G, Vasta G. Expression and secretion of galectins in the murine lung is modulated during influenza and pneumococcal infection. Society for Glycobiology Annual Meeting, November, 2011. Seattle, WA). PBS and heat-inactivated NA (ΔNA) (100°C, 15 min) were used as controls. The loss of catalytic activity in ΔNA was confirmed in a NA assay using 2'-(4-methylumbelliferyl)-α-D-N-acetylneuraminic acid sodium salt hydrate as a substrate (23). Animals were sacrificed the next day or at the indicated time points. BALF was collected for white blood cell count and cytokine determination, and the remaining lung tissues were either stored in TRIzol Reagent (Invitrogen) for RNA extraction, or processed to a cell suspension for flow cytometry analysis (see below). TNF-α, IL-1β, KC, LIX and MIP2 concentrations in BALF were determined with ELISA kits (R&D Systems).

Lung wet-to-dry weight ratio

To quantify the lung edema in ALI, whole lung tissue was collected, rinsed to remove surface blood, patted dry, and their immediate weights were recorded as the wet weight. The tissues were air dried for 3 days and their weights were recorded daily until they became stable and recorded as the dry weight. A wet/dry weight ratio for each individual mouse lung was calculated.

Lung Histology and H&E staining

After euthanasia, mouse thoracic cavities were opened to expose the trachea. Two sutures were placed around the top and bottom of trachea. An 18-gauge blunt needle was inserted at the top of the trachea with an incision, and tied with the top suture. About 2 ml of PREFER solution (Glyoxal fixative, Anatech Ltd.) was slowly perfused to dilate the lung tissue. After perfusion, the bottom trachea was closed by tying the suture. The lungs were dissected from the thoracic cavity and fixed in PREFER buffer overnight. Lung tissues were dehydrated, paraffin-embedded, and sectioned (8 μm). Some sections were stained with H&E; the remaining unstained sections were used for tissue lectin blots or TUNEL staining for apoptosis.

Lectin blot on tissue sections

The tissue sections were deparaffinated in xylene twice for 5 min and rehydrated in the serial ethanol solutions. The sections were washed in PBS, blocked in 3% BSA, incubated for 1 h with biotinylated PNA, SNA, or MAAII followed by streptavidin-conjugated Cy2 (a kind gift from Dr Adam C. Puche). The sections were counter-stained with DAPI and mounted with mounting medium for fluorescent microscopy. The images were captured on an Olympus BX61 Fluoview Laser Scanning Microscope with a 60X objective and 2.5X digital amplification with Fluoview V5.0. The images from different channels were merged with Adobe Photoshop 4.0.

TUNEL staining

The tissue sections were rehydrated as described above. Rehydrated tissue sections were treated with proteinase K (Roche Applied Science) for 30 min and washed twice with PBS.

The sections were stained with Fluorescein In Situ Cell Death Detection Kit (Roche Applied Science) per the manufacturer's recommendation, counter-stained with DAPI, and mounted for microscopic observation.

RNA extraction, reverse transcription, and qRT-PCR array

Total RNA from lung tissues was isolated with TRIzol reagent (Invitrogen) according to the manufacturer's recommendation. Total RNA (1 μg) was treated with 1 unit of DNase I (Invitrogen) in 10 μl reaction buffer for 15 min. DNase I was inactivated by addition of EDTA solution and heated at 65° C for 10 min. The treated RNA was reverse transcribed into cDNA using Reverse Transcriptase System (Promega) per the manufacturer's recommendation. The final products were diluted up to 100 μl with distilled water and 2 μl (from 0.02 μg of total RNA) was used for each PCR reaction. cDNA were mixed with SYBR mixer (Applied Biosystems) and 1 μM of each primer from the set of Mouse Cytokine Primer Library II (Real Time Primers, LLC) to a volume of 20 μl, and amplified in 7900HT Fast Real-Time PCR System (Applied Biosystems). Each sample was amplified in triplicate and average values were calculated. The relative gene expression level for each sample was normalized to HPRT.

Assay for Endothelial Barrier Function

Transendothelial ^{14}C-BSA flux was used as a measure of endothelial paracellular permeability as previously described (31). Briefly, gelatin-impregnated polycarbonate filters (13 mm diameter, 0.4 μm pore size; Nucleopore) mounted in chemotactic chambers (ADAPs, Dedham, MA) were inserted into wells of 24-well plates. Each upper compartment was seeded with HMVEC-Ls at 2.5×10^5 cells in 0.5 ml media per chamber and cultured for 72 h. The baseline barrier function of each monolayer was determined by applying ^{14}C-BSA to each upper compartment (0.5 ml) for 1 h at 37° C, after which the lower compartment (1.5 ml) was counted for ^{14}C activity. Only monolayers retaining ≥97% of the ^{14}C-BSA tracer were utilized. The monolayers were then exposed for 6 h to NA, ΔNA, LPS (300 ng/ml), or medium alone. In selected experiments, the HMVEC-L monolayers were preincubated for 1h with either NA or medium alone after which they were treated for 6h with LPS (30 ng/ml) or medium alone. In all experiments, transfer of ^{14}C-BSA across HMVEC-L monolayers was again assayed and expressed as pmol/h.

Flow cytometry

Cell suspensions from digested lung tissues were prepared as follows: after BALF wash, the lung was excised, minced into fine pieces, and digested in RPMI1640 (Invitrogen) containing 1 mg/ml of collagenase D (Roche), 10 μg/ml of DNase I (Invitrogen), 5 M of $CaCl_2$, and 1% of fetal bovine serum for 30 min at 37° C. The cell suspension was separated from tissue debris by passing it through a 40 μm mesh strainer and washed with PBS for staining. The cells were incubated for 1 h with 1) anti-human Surfactant Protein A (SurfA) antibody (Millipore) for airway epithelial cells, followed by 1 h incubation with Allophycocyanin (APC)-conjugated anti-rabbit IgG (BD Pharmingen), 2) anti-human CD31 (BD biosciences) for endothelial cells followed by APC conjugated anti-mouse IgG (BD Pharmingen), or 3) APC-conjugated anti-human CD11b (BD biosciences) for phagocytes. The cells undergoing apoptosis were detected with FITC-conjugated Annexin V Apoptosis Detection Kit (BD Pharmingen) according to manufacturer's recommendation, and analyzed on a Moflow cytomer/cell sorter (Daki-Cytomation). Briefly, the antibody-stained cells were washed twice with cold PBS and and resuspended in Binding Buffer (BD Pharmingen) at 1×10^6 cells/ml. 100 μl of cell suspension was transferred to a new tube with 5 ul of Annexin V-FITC solution and 5 ul of PI solution (BD Pharmingen) and incubated for 15 min before analysis. The cells that were stained PI-negative, but Annexin V-positive, were considered

to have undergone apoptosis; and the cells stained PI-positive were considered to be dead cells.

Statistical analysis

Multiple regression modeling and analysis of variance (ANOVA) were used in analyzing effects of NA, LPS, heat-inactivated NA, and Bcl-2 pretreatment on outcomes of interest. In regression modeling, effects of NA and LPS, as well as their interaction, were included initially; the absence of interaction suggests the effects of NA and LPS are additive, whereas the presence of an interaction suggests the effect of LPS depends on whether or not NA treatment was present. In ANOVA, we used the Tukey (or Tukey-Kramer) multiple comparisons procedure for pairwise comparisons of two or more treatments (32). P-values ≤ 0.05 were considered statistically significant. In a few instances we considered results suggestive of an effect even though the p-value was >0.05.

Results

NA desialylated the bronchioles and alveolar surface within 30 minutes

Airway epithelial cells are heavily sialylated (17, 18). However, the sialyl linkages from each anatomic section of the airway are species specific. Using lectin blot techniques established in our laboratory (33), we determined the sialylation status of murine lung tissues and their response to sialidase treatment. Lectins are a group of proteins that bind specifically to different glycoconjugates: SNA and MAA II recognize terminal sialic acids in α-2,6- or α-2,3-linkages, respectively, while PNA recognizes a subterminal β-galactose after terminal sialyl residues have been removed (33, 34). PBS (as untreated control) or NA (100 mU in 25 μl of PBS) was administered i.t. to mice, and 30 min later lung tissues were harvested and processed for lectin staining (green). SNA stained most of the alveolar areas in PBS-treated lung tissue (Figure 1a), and the SNA signal slightly decreased after NA treatment (Figure 1b); MAAII staining of the alveolar area was less intense (Figure 1c), but also diminished after NA treatment (Figure 1d). In PBS–treated tissues, PNA binding was found only on a few bronchi/bronchiole surfaces, likely indicative of sialyl residues masking underlying galactose molecules (Figure 1e). After NA treatment, robust PNA binding was found in bronchi, bronchioles, and some alveolar areas (Figure 1f). These combined data confirm that mouse lung tissues are sialylated with both α-2,6-linkage and, to a lesser degree, α-2,3-linkages, and that administration of clostridial NA, which is known to cleave both α-2,3- and α-2,6-glycosidic linkages (35), desialylated the bronchi, bronchioles, and alveolar areas, thereby exposing subterminal galactose residues on the surface of the airway epithelia.

Desialylation increased LPS-induced PMN recruitment and pulmonary edema formation

LPS administration into lung tissues provokes components of ALI in mice, including pulmonary leukostasis, edema, and increased inflammatory cytokine expression (28, 36). To study the effect of desialylation on PMN-dependent ALI, we pretreated mice with PBS, NA, or heat-inactivated NA (ΔNA) 30 min before LPS challenge (5 μg in 25 μl of PBS), and 18 h later, PMN counts in BALF were determined. As expected, mice treated with PBS and challenged with LPS (PBS/LPS) exhibited increased numbers of PMNs in BALF compared to mice who received PBS alone (PBS/PBS) ($p<0.0001$ by Tukey procedure, Figure 2A). NA treatment followed by PBS challenge (NA/PBS) produced only a slight increase in BALF PMN above the level of the PBS/PBS treatment group, but NA greatly increased BALF PMNs after LPS challenge (NA/LPS) compared to that observed with PBS/LPS ($p<0.0001$, Figure 2A). This NA-induced enhancement in BALF PMNs was not found using heat-inactivated NA (ΔNA/LPS) (Figure 2A), which confirmed the involvement of the heat-

labile NA catalytic activity. These data indicate that prior desialylation enhances the LPS-induced PMN recruitment into the bronchoalveolar compartment.

NA (NA/PBS) or LPS challenge (PBS/LPS) each alone increased the mean lung wet-to-dry weight ratio, a measure of lung edema, compared to PBS-treated mice (PBS/PBS) (Figure 2B). However, NA/LPS challenge further increased the mean wet-to-dry weight ratio compared to PBS/LPS (Figure 2B). In multiple linear regression modeling both the LPS ($p=0.009$) and NA effects ($p=0.002$) were independently significant, and the effects of NA and LPS appeared to be additive. These data indicate that prior desialylation further enhanced pulmonary edema formation in response to LPS challenge.

Next, we studied the histological changes in the lung tissue following LPS challenge in the presence or absence of NA pretreatment (Figure 2C). At 18 h following LPS i.t. challenge, PBS/LPS increased PMN recruitment to alveolar tissues panel i) compared to the PBS/PBS controls (panel i), but no damage to either endothelium or epithelium was evident. NA/PBS treatment did not induce histological changes compared to control PBS/PBS mice (Figure 2C, panel iii). However, PMN infiltration was dramatically increased in lung tissue after NA/LPS challenge (Figure 2C, panel iv). These findings are consistent with our results showing increased PMN infiltration from the BALF (Figure 2A).

Desialylation increased PMN recruitment in the absence of KC

KC, a murine functional homologue to human IL-8, is a potent PMN attractant and has been reported to be induced in lung tissue in an ALI model (35). We speculated that if the LPS-induced KC expression in lung tissues was further increased with NA pretreatment, it would potentiate PMN infiltration. Accordingly, we determined the KC concentration in the BALF 18 h after LPS challenge. Unexpectedly, although KC was increased after LPS challenge ($p<0.0001$ in linear regression), there was no apparent effect of NA, either with or without LPS challenge (Figure 3A). A similar result was obtained for 2 other chemotactic chemokines, LIX and MIP2 (Figure 3B). Heat-inactivated NA also had no apparent effect on KC (Figure 3A).

Because PMN recruitment into the lung was observed as early as 3 h after LPS challenge (data not shown), we analyzed chemokine expression in BALF at early time points following LPS challenge. Surprisingly, NA treatment alone appeared to increase KC biosynthesis and release within 30 min, the time point that immediately preceded LPS administration ($t=0$). This was based, however, on only 2 mice with and 2 mice without NA treatment observed before challenge ($p=0.097$). At 1 h after LPS challenge, the chemokine production from mice receiving NA pre-treatment only slightly surpassed chemokine levels in mice receiving PBS/LPS challenge. Although both NA pre-treatment and LPS challenge appeared to increase chemokine levels, at neither 1 h nor 3 h were treatments significantly different from each other by the Tukey multiple comparisons procedure, except for a significant increase ($p<0.05$) with NA/LPS treatment compared to the PBS/PBS control at 3 h (Figure 3C). LIX production at 3 h with NA/PBS treatment was similar to that observed after PBS/LPS challenge and with NA/LPS treatment. All showed significant increases ($p<0.01$) over the level with the PBS/PBS control (Figure 3D). Other chemokines, such as MIP2, also did not increase with NA pretreatment (data not shown). Thus, increased BALF PMNs associated with NA pretreatment could not be attributed to potentiation of chemokine protein expression.

To determine if KC played a role in PMN infiltration and/or increased PMNs in BALF, we challenged $KC^{-/-}$ mice with LPS, with or without NA pretreatment. After LPS challenge of PBS-pretreated $KC^{-/-}$ mice, a small amount of PMN infiltration was observed (Figure 3E), which was much lower than that observed in similarly treated wild-type C57BL/6 mice

(p=0.014). This emphasizes the critical role of KC in attracting PMNs into lung tissues during LPS-induced ALI. Nevertheless, even with minimal KC production, NA pretreatment combined with LPS challenge increased the PMN infiltration ($p<0.05$ by Tukey procedure for NA/LPS compared with PBS/PBS and NA/PBS; p=0.067 for NA/LPS compared with PBS/LPS) (Figure 3E). These results suggest that prior desialylation can partially increase PMN recruitment to the BALF through a KC-independent mechanism.

NA treatment alters expression of multiple genes

Although treatment with NA alone induced KC and LIX production (Figure 3B-D), it only slightly increased PMNs in BALF (Figure 2A). These findings suggest that elevation of these chemokines alone was insufficient to explain the increased PMN recruitment in response to LPS challenge after NA pretreatment. To determine the alteration of inflammatory cytokine/chemokine gene expression in lung tissue after desialylation, we carried out a RealTime PCR array and compared inflammatory gene expression in the lung homogenates after 30 min of NA treatment. Heat-inactivated NA was used as the untreated control to offset any stimulation effect by potential contaminants in the NA preparation. In comparison to heat-inactivated NA-treated tissues, 9 of 88 genes (http://www.realtimeprimers.com/mocyprliii.html) were upregulated, mostly chemokines, while expression of one chemokine gene, CCL27, was down-regulated with desialylation (Figure 4A). In addition to the chemokines, TNF-α was up-regulated as we previously reported (7).

TNF-α, a major inflammatory cytokine produced in response to LPS stimulation, can activate endothelial cells (22). We therefore measured the effect of NA pretreatment on LPS-induced TNF-α protein production in BALF. NA treatment alone appeared to increase TNF-α protein production within 30 min (p=0.094 for 2 mice with and 2 mice without NA pretreatment, Figure 4B). At 1 h after LPS challenge, there was higher TNF-α production with LPS challenge, with or without NA pretreatment, than in PBS/PBS controls, but none of the differences were statistically significant. At 3 h, there was increased production with LPS challenge compared to treatment with PBS, but no differences among treatments were statistically significant (Figure 4B). NA pretreatment with LPS challenge increased IL-1β production in the lung (supplementary Figure S1A); however, LPS-induced PMN infiltration was increased with NA pretreatment in caspase-1-deficient mice and IL-1R1 knockout mice (supplementary Figure S1B-C), which lack functional IL1β and its receptor, respectively. This suggests that despite increased IL-1β expression, IL-1β and its signaling pathway may not be critical for LPS-induced PMN infiltration.

NA treatment disrupted endothelial barrier integrity

As TNF-α, which was upregulated by NA treatment (Figure 4A), has the capability to increase endothelial paracellular permeability (22, 31), we asked whether prior desialyation increases PMN recruitment to BALF through opening of the endothelial paracellular pathway. To address this question, we treated post-confluent HMVEC-L monolayers with NA and measured transendothelial flux of ^{14}C labeled-BSA (31). While LPS treatment increased BSA flux ($p<0.05$ compared to each of the other treatments by the Tukey multiple comparisons procedure), there was no evidence of barrier disruption after treatment with a high concentration of NA alone (100 mU/ml), compared to treatment with medium alone or heat-inactivated NA (Figure 5A).

We then asked whether NA pretreatment was able to enhance endothelial barrier responsiveness to LPS stimulation. For this purpose, a concentration of LPS (30 ng/ml), which alone did not induce EC permeability, was used. Indeed, NA pretreatment combined with a subthreshold LPS exposure stimulation increased transendothelial ^{14}C-albumin flux

($p< 0.001$ by the Tukey procedure for NA+LPS compared to all other treatments, Figure 5B).

Since EC apoptosis could underlie the observed loss of barrier function, we next studied if NA pretreatment, alone or in combination with LPS, increased HMVEC-L apoptosis. The ECs were suspended and stained with Annexin V and Propidium Iodide (PI) for flow cytometry analysis. While LPS alone did not induce more apoptotic cells, NA treatment alone induced cellular apoptosis. Moreover, NA treatment plus LPS induced even more apoptotic cells (Figure 5C). In contrast, while LPS stimulation induced TNF-α production in EC culture supernatant ($p<0.01$ compared to medium), NA treatment alone did not (Figure 5D). However, NA/LPS treatment induced more TNF-α than LPS alone in this *in vitro* system ($p<0.01$, Figure 5D), as it did *in vivo* (Figure 4B). These data suggest that desialylation of ECs potentiates LPS-induced apoptosis, which may contribute to ALI, perhaps in part through a TNF-α-mediated mechanism. However, while administration of anti-TNF-α antibody reduced TNF-α levels in the BALF, it did not reduce the increased PMN infiltration of NA/LPS challenged mice (Supplementary Figure S2), which suggests a TNF-α independent mechanism is involved.

Desialylation increased the apoptosis in lung tissue after LPS challenge

Since TNF-α is associated with cellular apoptosis (36-38) and was induced by LPS challenge (Figure 4), we asked whether apoptosis was induced in lung tissues after LPS challenge, and, if so, whether such LPS-induced apoptosis could be enhanced by prior desialylation. Lung tissues from mice after overnight LPS challenge were sectioned and TUNEL-stained. As expected, while PBS/PBS treated lung showed minimal apoptosis (Figure 6A, panel i), the PBS/LPS challenge increased cellular apoptosis (Figure 6A, panel ii). Scattered apoptotic cells were identified in tissues treated with NA/PBS (Figure 6A, panel iii); however, NA/LPS challenge induced a greater amount of cellular apoptosis (Figure 6A, panel iv), which is more apparent than that following PBS/LPS treatment (Figure 6A, panel ii).

To quantify the degree of apoptosis in lung tissue, we prepared single cell suspensions from the whole lung tissue and performed flow cytometry analysis with Annexin V-PI staining, the latter being a measure of dead cells. The cells that were stained PI-negative, but Annexin V-positive, were considered to have undergone apoptosis. In control lung (PBS/PBS), 8.7% of total cells were apoptotic (0.37×10^6 cells), while from PBS/LPS challenged mice, 15.7 % were apoptotic cells (1.51×10^6, $p<0.05$ compared to PBS/PBS). In NA/LPS challenged mice, the percentage of apoptotic cells increased to 21.8% (2.28×10^6, $p<0.01$ *vs.* PBS/LPS) (Figure 6B). These data correlated with tissue TUNEL staining (Figure 6A). Further analysis indicated that a higher percentage of cells in the $SurfA^+$, myeloid ($CD11b^+$), and endothelial ($CD31^+$) cell populations were undergoing apoptosis with NA/LPS challenge than with PBS/LPS challenge; however, the difference between counts with NA/LPS challenge and PBS/LPS challenge was statistically significant only for $CD11b^+$ (Figure 6B).

Recombinant human Bcl-2 suppressed NA-induced increase in PMN infiltration

We considered that the increased in apoptosis with NA pre-treatment could account for the increased PMNs in the BALF, increased pulmonary edema, and diminished EC barrier function *in vitro*. We speculated that inhibition of apoptosis by addition of exogenous Bcl-2 would counteract the NA effect on LPS-induced lung injury. Bcl-2 is an anti-apoptotic agent that can neutralize pro-apoptotic activity and prevent cell death (39, 40). Mice were administered 1 μg of recombinant human Bcl-2 (rhBcl-2) or saline (as mock control) i.p. 30 min before NA treatment (I.t.), followed by LPS challenge to evaluate the effect of anti-apoptosis treatment on LPS-induced ALI. With PBS/LPS challenge (open bars), there was a

small, not statistically significant, difference in BALF infiltration between saline and rhBcl-2-treated mice. In the saline pretreatment group, while NA/LPS (closed bars) induced more PMN infiltration than in mice given PBS/ LPS challenge ($p<0.05$ by Tukey test) (Figure 7A), by contrast, in the presence of rhBcl-2, PMN infiltration following NA/LPS challenge was lower than the level seen with NA/LPS in the absence of rhBcl-2 and was also lower than the level observed after PBS/LPS challenge (Figure 7A).

To determine whether rhBcl-2 treatment reversed another measure of ALI, pulmonary edema, we measured wet-to-dry weight ratios in mice that were treated with either saline or rhBcl-2 before PBS/LPS or NA/LPS challenge (Figure 7B). Compared to PBS/PBS, LPS challenge alone (PBS/LPS) induced higher wet-to-dry weight ratios in mice pretreated with either saline or rhBcl-2. As with PMN infiltration, an increase in wet-to-dry ratio was seen with NA/LPS challenge compared to PBS/LPS challenge with saline pretreatment ($p<0.05$ by Tukey test) but not with rhBcl-2 pretreatment.

As Bcl-2 pretreatment reversed the enhanced PMN infiltration and wet-to-dry ratio in lungs with NA/LPS challenge, we wondered if this was associated with suppression of NA-induced apoptosis in lung tissue. Therefore, we pretreated mice with saline or rhBcl-2 before PBS/LPS or NA/LPS challenge, harvested the single cell suspension from the lung, and quantified the amount of apoptotic cells (Figure 7C). With either prior saline or prior rhBcl-2 infusion, the NA/LPS-challenged mice had more apoptotic cells than those challenged with PBS/LPS ($p<0.001$ for NA/LPS compared to PBS/LPS with saline, $p < 0.05$ for NA/LPS compared to PBS/LPS with rhBcl-2). As with PMN infiltration and wet-to-dry ratio, the level for NA/LPS was lower with prior rhBcl-2 than with prior saline, but the difference was not statistically significant. These results are consistent with the hypothesis that Bcl-2 inhibits the NA-mediated apoptosis in lung tissue.

We further analyzed the effect of Bcl-2 on apoptosis in endothelial ($CD31^+$), epithelial ($SurfA^+$), and myeloid ($CD11b^+$) populations (Figure 7D). With prior saline treatment, the number of apoptotic cells increased in all populations with NA treatment ($p<0.0001$ for $CD11b^+$, $p=0.0002$ for $CD31^+$, $p=0.077$ for SurfA). On the other hand Bcl-2 pre-treatment appeared to decrease the number of apoptotic cells in the $CD11b^+$ ($p=0.032$) population but not for the $CD31^+$ ($p=0.063$) and $SurfA^+$ ($p>0.50$) populations.

Taken together, these data suggest that the desialylation-mediated increase of LPS-induced PMN infiltration and pulmonary edema are dependent in part on apoptosis and can be ameliorated by the administration of anti-apoptotic agents such as Bcl-2, while the LPS-induced PMN infiltration may involve additional mechanisms, such as the opening of the endothelial paracellular pathway

Discussion

The airway epithelial cell surface is armed with numerous receptors that recognize host mediators and exogenous danger signals. Many of these receptors contain oligosaccharide chains whose outermost positions terminate with sialic acid. These highly electronegative, hydrophilic sialyl residues influence protein tertiary conformation, and in their terminal location are strategically positioned to influence intermolecular and cell-cell interactions through steric hindrance and/or electrostatic repulsion. Further, these sialyl residues may mask “activation epitopes” as we have reported for β2 integrin and the TLR4 receptor complex (21, 32). The current studies support the hypothesis that removal of sialyl residues from lung tissue potentiates LPS-induced acute lung injury through enhanced PMN recruitment and transendothelial migration, proinflammatory cytokine and chemokine production, pulmonary edema formation, and apoptosis.

Mammalian lung tissues are sialylated with both α-2,6-linked, and less consistently, α-2,3-linked sialic acids (17, 18, 42, 43). Our data confirmed the presence of α-2,6-linked sialic acid and to a lesser extent, α-2,3-linked sialic acid in CD1 outbred mouse lungs (Figure 1). PNA lectin binding to lung tissue was increased following i.t. installation of exogenous NA, thereby confirming the loss of sialyl residues (Figure 1).

Of note, while desialylation upregulated gene expression in lung tissue, including genes encoding for certain chemokines and TNF-α (Figure 4), in the absence of LPS challenge, NA treatment did not cause acute lung injury as measured by PMNs in the BALF (Figure 2); however, this desialylation-induced "reprogramming" of the lung tissues dramatically altered the responses to LPS challenge (Figure 2, 6). It is possible that mucosal pathogens that express a sialidase may induce a similar desialylation-induced reprogramming of lung tissue. If that were the case, then the pulmonary innate immune responses to subsequent pathogens or endogenous alarmins could be similarly altered.

PMN recruitment into inflamed tissues is a critical step in the host innate immune response. This multistep process is tightly orchestrated to diminish collateral tissue damage. To initiate PMN transmigration through the endothelium, endothelial cell activation is required, either directly, as with exposure to LPS, or indirectly, through the induction of cytokines. This leads to *de novo* synthesis and surface expression of adhesion molecules (44, 45). The interactions between the selectins on "inflamed" endothelium and their counter-ligands on PMNs slow the circulating cells, enabling firm adhesion through the interactions between activated ICAMs and integrins. The induced firm adhesion enables the PMNs to transmigrate through the endothelial cell-cell junction down a chemokine gradient toward the inflamed site (44, 45).

In the current study, the increased protein content of KC, MIP-2, LIX, and TNF-α in BALF was evident after LPS challenge (Figures 3, 4, 5). KC is a critical chemokine that locally attracts PMNs into tissues (29, 46, 47). Its importance in LPS-provoked PMN recruitment is clear, based on the observation that the LPS-induced PMN infiltration is nearly absent in $KC^{-/-}$ mice (Figure 3C). In the absence of KC, other redundant chemokines, such as MIP-2 and LIX, might contribute to PMN recruitment into lung tissues. However these two chemokines are less potent chemotactically than KC (IL-8) (47). Since NA treatment alone upregulated expression of KC and other chemokines, but failed to increase PMN infiltration in lung tissues without a subsequent LPS challenge, these chemokines alone may be insufficient to attract PMNs into lung tissue in our murine model of ALI (Figure 4). Further, the enhanced LPS-induced PMN infiltration with NA pretreatment was not simply due to elevated KC or other chemokines (MIP-2, LIX) production because the concentration of these chemokines from LPS-challenged mice with NA pretreatment did not differ substantially from those without NA treatment (Figure 3). Therefore, elevation of these PMN-attracting chemokines alone cannot explain the increased cell infiltration with NA pretreatment followed by LPS challenge. On the other hand, in the absence of KC, the minimal PMN infiltration was still enhanced with NA pretreatment (Figure 3E). LPS induces inflammatory cytokine expression such as TNF-α, IL-6 and IL-8 (19, 36, 48) in endothelial cells that can upregulate its surface expression of E-selectin and ICAM-1 (49-51), adhesion molecules important in leukocyte infiltration. In addition, monocytes, macrophages, dendritic and epithelial cells in the lung each produce proinflammatory cytokines in response to LPS stimulation (19, 20). In LPS-induced ALI, intrapulmonary cytokine expression is upregulated at the protein (Figure 4B, Figure S1) level. As TNF-α is induced in lung tissue and is capable of activating endothelial cells, it likely contributes to the LPS-induced PMN infiltration, as we previously reported (22); however, neutralizing anti-TNF-α antibodies did not reduce PMN recruitment (Figure S2). In contrast, another pro-inflammatory cytokine, IL-1β, which is capable of activating endothelial cells and

inducing neutrophilia, was also expressed after LPS administration, but, based on experiments in caspase-1 and IL-1R-deficient mice, did not appear to contribute to PMN infiltration in our model of LPS-induced lung injury (supplemental data).

Given the prevalence of sialylated glycoconjugates on the surface of mammalian cells, including lung tissue, there is a large array of potential molecular targets for NA. We reported previously that desialylation of monocytes *in vitro* activated phosphorylation of ERKs and induced cytokine production in response to LPS (19). In a subsequent publication, we demonstrated that removal of sialyl residues from the TLR4 receptor complex accelerated and enhanced LPS-initiated signaling (21). Further, removal of sialyl residues led to activation of PMN β2 integrins and enhanced adhesion, while desialylation of ICAM-1 promoted leukocyte arrest in an *in vivo* model of cell migration (33). Recently, we reported that MUC1 and the EGF receptor on airway epithelial cells were highly sialylated and that desialylation enhanced their responsiveness to their cognate ligands (52). Thus, desialylation of cell surface glycoconjugate molecules relevant to ALI potentiated inflammatory responses to LPS.

The molecular mechanism(s) by which desialylation enhanced LPS-mediated ALI remains to be determined. Edema (wet-to-dry weight) in lung tissues, suggestive of loss of endothelial barrier function, was induced after LPS challenge and was enhanced upon desialylation (Figures 2B&7). Consistent with this observation, LPS increased endothelial permeability *in vitro*, and NA pretreatment lowered the threshold at which LPS induced endothelial permeability (Figure 5).

An earlier investigation showed that LPS-induced vascular collapse resulted from disseminated endothelial apoptosis mediated sequentially by the generation of TNF-α and ceramide (53) The disseminated endothelial apoptosis preceded nonendothelial parenchymal tissue damage. It is possible that desialylation potentiated the TLR4 receptor complex-mediated signaling, as we recently reported (21). This might result in the enhanced expression of TNF-α and/or ceramide. Alternatively, desialylation of proteins located at the interendothelial cell junction could contribute to the ALI. Endothelial cell adherens junction proteins, such as VE-cadherin, are sialylated, and could be an additional target of NA (54). It is likely that the NA-associated increase in endothelial “leak” contributes to the leukocyte infiltration.

LPS administration induced ALI as measured by recruitment of PMNs to the BALF and increased wet-to-dry weight in the lungs, a measure of pulmonary edema. These effects were substantially increased by NA pretreatment and were accompanied by apoptosis, as evidenced by both TUNEL and Annexin V staining (Figure 6). The exogenous administration of the anti-apoptosis reagent, recombinant human Bcl-2, abolished the NA treatment effect, but interestingly, did not ameliorate the ALI induced by LPS alone (Figure 7). This observation suggests that there may be two apparently distinct and independent signaling mechanisms by which NA and LPS induce apoptosis. Since NA treatment can induce apoptosis in the absence of causing endothelial barrier dysfunction (Figure 5), apoptosis alone cannot explain the development of acute lung injury. In our murine model, a “second hit”, as provided by LPS to either enlist additional pathogenic mechanisms or to increase the level of apoptosis above that induced by NA alone appears to be required for the development of acute lung injury.

The anti-apoptotic protein, Bcl-2, is a member of a larger family of Bcl-2 intracellular proteins that may be released extracellularly during cecal ligation and puncture-induced sepsis (55) or during cell necrosis. In previous studies, treatment of mice with rhBcl-2 protected them from sepsis by reducing apoptosis in multiple target tissues (56), including

endothelial cells (41). Bcl-2 inhibits ceramide-mediated apoptosis (53) Thus, extracellular Bcl-2 may be considered a DAMP (damage-associated molecular pattern) or alarmin that modulates the response of the innate immune system to tissue injury (40). Administration of rhBCL2A1 to mice also increased expression of endogenous Bcl-2 protein in mice and was associated with increased recruitment of PMNs to the inflammatory site, but not the induction of pro-inflammatory cytokines (56). Most likely, LPS-induced PMN infiltration is an active mechanism mediated predominantly by IL-8 (KC in mice) and is apoptosis-independent, whereas desialylation triggers another pathway that is apoptosis-dependent, but KC-independent, which additively enhances the PMN infiltration in response to LPS. This is consistent with our observation that NA pretreatment was able to increase LPS-induced PMN recruitment even in the absence of KC (Figure 3E).

Microbial NAs could be important for the pathogenesis of infection, particularly for those agents that target mucosal surfaces (24, 26, 57). Thus, mucosal surfaces are likely to be desialylated during or after infection, and this may increase the likelihood of further lung injury or susceptibility to secondary infection. Indeed, we have recently shown that non-lethal infection of mice with influenza results in greatly increased severity of *S. pneumonae* infection (58). Further, host-derived sialidases, or NEU proteins, the NA homolog present in myeloid, epithelial and endothelial cells, may play an important role in cellular function by desialylating MUC1 or EGFR, or other surface glycoconjugate receptors (23, 52). Therefore, it is important that the role of sialidases in the host immune response to infections be better defined. Such studies may lead to novel therapeutic applications of neuraminidase inhibitors, including a more expansive role in treating pulmonary hyperinflammatory conditions.

Supplementary Material

Refer to Web version on PubMed Central for supplementary material.

Acknowledgments

These studies were supported by NIH grant HL086933-01A1 to ASC, AI018797 to SV, and HL089179 to SEG.

References

1. Daniels MA, Devine L, Miller JD, Moser JM, Lukacher AE, Altman JD, Kavathas P, Hogquist KA, Jameson SC. CD8 binding to MHC class I molecules is influenced by T cell maturation and glycosylation. Immunity. 2001; 15:1051–1061. [PubMed: 11754824]
2. da Silva Correia J, Ulevitch RJ. MD-2 and TLR4 N-linked glycosylations are important for a functional lipopolysaccharide receptor. J Biol Chem. 2002; 277:1845–1854. [PubMed: 11706042]
3. Diamond MS, Staunton DE, Marlin SD, Springer TA. Binding of the integrin Mac-1 (Cd11b/cd18) to the 3rd immunoglobulin-like domain of Icam-1 (Cd54) and its regulation by glycosylation. Cell. 1991; 65:961–971. [PubMed: 1675157]
4. Baba M, Yong Ma B, Nonaka M, Matsuishi Y, Hirano M, Nakamura N, Kawasaki N, Kawasaki N, Kawasaki T. Glycosylation-dependent interaction of Jacalin with CD45 induces T lymphocyte activation and Th1/Th2 cytokine secretion. J Leukoc Biol. 2007; 81:1002–1011. [PubMed: 17242371]
5. Kurayoshi M, Yamamoto H, Izumi S, Kikuchi A. Post-translational palmitoylation and glycosylation of Wnt-5a are necessary for its signalling. Biochem J. 2007; 402:515–523. [PubMed: 17117926]
6. Ohnishi T, Muroi M, Tanamoto K. MD-2 is necessary for the toll-like receptor 4 protein to undergo glycosylation essential for its translocation to the cell surface. Clin Vaccine Immunol. 2003; 10:405–410.
7. Gleeson PA. The sweet side of immunology: glycobiology of the immune system. Immunol Cell Biol. 2008; 86:562–563. [PubMed: 18830249]

8. Ma BY, Mikolajczak SA, Yoshida T, Yoshida R, Kelvin DJ, Ochi A. CD28 T cell costimulatory receptor function is negatively regulated by N-linked carbohydrates. Biochem Biophys Res Commun. 2004; 317:60–67. [PubMed: 15047148]
9. Christie DR, Shaikh FM, Lucas JA 4th, Lucas JA 3rd, Bellis SL. ST6Gal-I expression in ovarian cancer cells promotes an invasive phenotype by altering integrin glycosylation and function. J Ovarian Res. 2008; 1:3.10.1186/1757-2215-1-3 [PubMed: 19014651]
10. Rifat S, Kang TJ, Mann D, Zhang L, Puche AC, Stamatos NM, Goldblum SE, Brossmer R, Cross AS. Expression of sialyltransferase activity on intact human neutrophils. J Leukoc Biol. 2008; 84:1075–1081. [PubMed: 18664529]
11. Schauer R. Sialic acids and their role as biological masks. Trends Biochem Sci. 1985; 10:357–360.
12. Kearse K, Cassatt D, Kaplan A, Cohen D. The requirement for surface Ig signaling as a prerequisite for T cell: B cell interactions. A possible role for desialylation. The Journal of Immunology. 1988; 140:1770–1778. [PubMed: 3126236]
13. Hayes G, Lockwood D. The role of cell surface sialic acid in insulin receptor function and insulin action. J Biol Chem. 1986; 261:2791–2798. [PubMed: 3512542]
14. Bridges K, Harford J, Ashwell G, Klausner R. Fate of receptor and ligand during endocytosis of asialoglycoproteins by isolated hepatocytes. Proc Natl Acad Sci U S A. 1982; 79:350–354. [PubMed: 6281767]
15. Hasegawa T, Yamaguchi K, Wada T, Takeda A, Itoyama Y, Miyagi T. Molecular cloning of mouse ganglioside sialidase and its increased expression in Neuro2a cell differentiation. J Biol Chem. 2000; 275:8007–8015. [PubMed: 10713120]
16. Fogel M, Altevogt P, Schirrmacher V. Metastatic potential severely altered by changes in tumor cell adhesiveness and cell-surface sialylation. J Exp Med. 1983; 157:371–376. [PubMed: 6848622]
17. Nicholls JM, Bourne AJ, Chen H, Guan Y, Peiris J. Sialic acid receptor detection in the human respiratory tract: evidence for widespread distribution of potential binding sites for human and avian influenza viruses. Respir Res. 2007; 8:73.10.1186/1465-9921-8-73 [PubMed: 17961210]
18. Ning ZY, Luo MY, Qi WB, Yu B, Jiao PR, Liao M. Detection of expression of influenza virus receptors in tissues of BALB/c mice by histochemistry. Vet Res Commun. 2009; 33:895–903. [PubMed: 19662506]
19. Stamatos NM, Curreli S, Zella D, Cross AS. Desialylation of glycoconjugates on the surface of monocytes activates the extracellular signal-related kinases ERK 1/2 and results in enhanced production of specific cytokines. J Leukoc Biol. 2004; 75:307–313. [PubMed: 14634064]
20. Stamatos NM, Carubelli I, van de Vlekkert D, Bonten EJ, Papini N, Feng C, Venerando B, d'Azzo A, Cross AS, Wang LX. LPS-induced cytokine production in human dendritic cells is regulated by sialidase activity. J Leukoc Biol. 2010; 88:1227–1239. [PubMed: 20826611]
21. Feng C, Stamatos NM, Dragan AI, Medvedev A, Whitford M, Zhang L, Song C, Rallabhandi P, Cole L, Nhu QM, Vogel SN, Geddes CD, Cross AS. Sialyl Residues Modulate LPS-mediated Signaling through the Toll-like Receptor 4 Complex. PloS One. 2012; 7:e32359.10.1371/journal.pone.0032359 [PubMed: 22496731]
22. Sakarya S, Rifat S, Zhou J, Bannerman DD, Stamatos NM, Cross AS, Goldblum SE. Mobilization of neutrophil sialidase activity desialylates the pulmonary vascular endothelial surface and increases resting neutrophil adhesion to and migration across the endothelium. Glycobiology. 2004; 14:481–494. [PubMed: 15044387]
23. Cross AS, Sakarya S, Rifat S, Held TK, Drysdale BE, Grange PA, Cassels FJ, Wang LX, Stamatos N, Farese A. Recruitment of Murine Neutrophils in Vivo through Endogenous Sialidase Activity. J Biol Chem. 2003; 278:4112–4120. [PubMed: 12446694]
24. Wagner R, Matrosovich M, Klenk HD. Functional balance between haemagglutinin and neuraminidase in influenza virus infections. Rev Med Virol. 2002; 12:159–166. [PubMed: 11987141]
25. Bonten E, van der Spoel A, Fornerod M, Grosveld G, d'Azzo A. Characterization of human lysosomal neuraminidase defines the molecular basis of the metabolic storage disorder sialidosis. Genes Dev. 1996; 10:3156–3169. [PubMed: 8985184]

26. Soong G, Muir A, Gomez MI, Waks J, Reddy B, Planet P, Singh PK, Kanetko Y, Wolfgang MC, Hsiao YS. Bacterial neuraminidase facilitates mucosal infection by participating in biofilm production. J Clin Invest. 2006; 116:2297–2305. [PubMed: 16862214]
27. Marini J, Evans T. Round table conference: acute lung injury. Intensive Care Med. 1998; 24:878–883. [PubMed: 9757935]
28. Matute-Bello G, Frevert CW, Martin TR. Animal models of acute lung injury. American Journal of Physiology- Lung Cellular and Molecular Physiology. 2008; 295:L379–L399.10.1152/ajplung.00010.2008 [PubMed: 18621912]
29. Shea-Donohue T, Thomas K, Cody MJ, Aiping Z, Detolla LJ, Kopydlowski KM, Fukata M, Lira SA, Vogel SN. Mice deficient in the CXCR2 ligand, CXCL1 (KC/GRO-alpha), exhibit increased susceptibility to dextran sodium sulfate (DSS)-induced colitis. Innate Immun. 2008; 14:117–124. [PubMed: 18713728]
30. Chen WH, Kang TJ, Bhattacharjee AK, Cross AS. Intranasal administration of a detoxified endotoxin vaccine protects mice against heterologous Gram-negative bacterial pneumonia. Innate Immunity. 2008; 14:269–278. [PubMed: 18809651]
31. Goldblum SE, Ding X, Campbell-Washington J. TNF-alpha induces endothelial cell F-actin depolymerization, new actin synthesis, and barrier dysfunction. Am J Physiol. 1993; 264:C894–905. [PubMed: 8476021]
32. Tukey JW. The philosophy of multiple comparisons. Statist Sci. 1991; 6:100–116.
33. Feng C, Zhang L, Almulki L, Faez S, Whitford M, Hafezi-Moghadam A, Cross AS. Endogenous PMN sialidase activity exposes activation epitope on CD11b/CD18 which enhances its binding interaction with ICAM-1. J Leukoc Biol. 2011; 90:313–321. [PubMed: 21551251]
34. Abe Y, Smith CW, Katkin JP, Thurmon LM, Xu XD, Mendoza LH, Ballantyne CM. Endothelial alpha 2,6-linked sialic acid inhibits VCAM-1-dependent adhesion under flow conditions. Journal of Immunology. 1999; 163:2867–2876.
35. Drzeniek R. Substrate specificity of neuraminidases. Histochem J. 1973; 5:271–290. [PubMed: 4593596]
36. Jeyaseelan S, Chu HW, Young SK, Worthen GS. Transcriptional profiling of lipopolysaccharide-induced acute lung injury. Infect Immun. 2004; 72:7247–56. [PubMed: 15557650]
37. Van Antwerp DJ, Martin SJ, Kafri T, Green DR, Verma IM. Suppression of TNF-alpha-induced apoptosis by NF-kappa B. Science. 1996; 274:787–789. [PubMed: 8864120]
38. Zychlinsky A, Fitting C, Cavaillon J, Sansonetti P. Interleukin 1 is released by murine macrophages during apoptosis induced by Shigella flexneri. J Clin Invest. 1994; 94:1328–1332. [PubMed: 8083373]
39. Hogquist K, Nett M, Unanue E, Chaplin D. Interleukin 1 is processed and released during apoptosis. Proc Natl Acad Sci U S A. 1991; 88:8485–8849. [PubMed: 1924307]
40. Iwata A, Morgan-Stevenson V, Schwartz B, Liu L, Tupper J, Zhu X, Harlan J, Winn R. Extracellular BCL2 proteins are danger-associated molecular patterns that reduce tissue damage in murine models of ischemia-reperfusion injury. PloS One. 2010; 5:e9103.10.1371/journal.pone.0009103 [PubMed: 20161703]
41. Karsan A, Yee E, Harlan JM. Endothelial cell death induced by tumor necrosis factor-alpha is inhibited by the Bcl-2 family member, A1. J Biol Chem. 1996; 271:27201–27204. [PubMed: 8910286]
42. Martin LT, Marth JD, Varki A, Varki NM. Genetically altered mice with different sialyltransferase deficiencies show tissue-specific alterations in sialylation and sialic acid 9-O-acetylation. J Biol Chem. 2002; 277:32930–32938. [PubMed: 12068010]
43. Glaser L, Conenello G, Paulson J, Palese P. Effective replication of human influenza viruses in mice lacking a major [alpha] 2, 6 sialyltransferase. Virus Res. 2007; 126:9–18. [PubMed: 17313986]
44. Langer HF, Chavakis T. Leukocyte–endothelial interactions in inflammation. J Cell Mol Med. 2009; 13:1211–1220. [PubMed: 19538472]
45. Zarbock A, Ley K. Neutrophil adhesion and activation under flow. Microcirculation. 2009; 16:31–42. [PubMed: 19037827]

46. Lin M, Carlson E, Diaconu E, Pearlman E. CXCL1/KC and CXCL5/LIX are selectively produced by corneal fibroblasts and mediate neutrophil infiltration to the corneal stroma in LPS keratitis. J Leukoc Biol. 2007; 81:786–792. [PubMed: 17110418]
47. Rovai LE, Herschman HR, Smith JB. The murine neutrophil-chemoattractant chemokines LIX, KC, and MIP-2 have distinct induction kinetics, tissue distributions, and tissue-specific sensitivities to glucocorticoid regulation in endotoxemia. J Leukoc Biol. 1998; 64:494–502. [PubMed: 9766630]
48. O'Grady NP, Preas HL, Pugin J, Fiuza C, Tropea M, Reda D, Banks SM, Suffredini AF. Local inflammatory responses following bronchial endotoxin instillation in humans. American Journal of Respiratory and Critical Care Medicine. 2001; 163:1591–1598. [PubMed: 11401879]
49. Wyble CW, Hynes KL, Kuchibhotla J, Marcus BC, Hallahan D, Gewertz BL. TNF-alpha and IL-1 upregulate membrane-bound and soluble E-selectin through a common pathway. J Surg Res. 1997; 73:107–112. [PubMed: 9441802]
50. Min W, Pober JS. TNF initiates E-selectin transcription in human endothelial cells through parallel TRAF-NF-kappa B and TRAF-RAC/CDC42-JNK-c-Jun/ATF2 pathways. J Immunol. 1997; 159:3508–3518. [PubMed: 9317150]
51. Myers CL, Wertheimer SJ, Schembri-King J, Parks T, Wallace RW. Induction of ICAM-1 by TNF-alpha, IL-1 beta, and LPS in human endothelial cells after downregulation of PKC. Am J Physiol. 1992; 263:C767–772. [PubMed: 1357985]
52. Lillehoj EP, Hyun SW, Feng C, Zhang L, Liu A, Guang W, Nguyen C, Luzina IG, Atamas SP, Passaniti A, Twaddell WS, Puche AC, Wang LX, Cross AS, Goldblum SE. NEU1 sialidase expressed in human airway epithelia regulates epidermal growth factor receptor (EGFR) and MUC1 protein signaling. J Biol Chem. 2012; 287:8214–8231. [PubMed: 22247545]
53. Haimovitz-Friedman A, Cordon-Cardo C, Bayoumy S, Garzotto M, McLoughlin M, Gallily R, Edwards CK 3rd, Schuchman EH, Fuks Z, Kolesnick R. Lipopolysaccharide induces disseminated endothelial apoptosis requiring ceramide generation. J Exp Med. 1997; 186:1831–1841. [PubMed: 9382882]
54. Geyer H, Geyer R, Odenthal-Schnittler M, Schnittler HJ. Characterization of human vascular endothelial cadherin glycans. Glycobiology. 1999; 9:915–925. [PubMed: 10460833]
55. Iwata A, Stevenson VM, Minard A, Tasch M, Tupper J, Lagasse E, Weissman I, Harlan JM, Winn RK. Over-expression of Bcl-2 provides protection in septic mice by a trans effect. J Immunol. 2003; 171:3136–3141. [PubMed: 12960340]
56. Iwata A, de Claro RA, Morgan-Stevenson VL, Tupper JC, Schwartz BR, Liu L, Zhu X, Jordan KC, Winn RK, Harlan JM. Extracellular administration of BCL2 protein reduces apoptosis and improves survival in a murine model of sepsis. PLoS One. 2011; 6:e14729.10.1371/journal.pone.0014729 [PubMed: 21390214]
57. Bouvier NM, Palese P. The biology of influenza viruses. Vaccine. 2008; 26:D49–D53. [PubMed: 19230160]
58. Chen WH, Toapanta FR, Shirey KA, Zhang L, Giannelou A, Page C, Frieman MB, Vogel SN, Cross AS. Potential role for alternatively activated macrophages in the secondary bacterial infection during recovery from influenza. Immunol Lett. 2012; 141:227–234. [PubMed: 22037624]

Abbreviations used in this paper

BALF	broncho-alveolar lavage fluid
PMN	polymorphonuclear leukocyte
NA	neuraminidase
ALI	acute lung injury
i.t.	intratracheally
rhBcl-2	recombinant human Bcl-2

PNA	Peanut Agglutinin
SNA	Sambucus Nigra Lectin
MAAII	Maackia Amurensis Lectin II
APC	Allophycocyanin
SurfA	Surfactant Protein A
ΔNA	heat-inactivated NA
PBS/PBS	PBS i.t. followed by PBS i.t. administration
PBS/LPS	PBS i.t. followed by LPS i.t. administration
NA/PBS	NA i.t. followed by PBS i.t. administration
NA/LPS	NA i.t. followed by LPS i.t. administration
PI	Propidium Iodide
EC	endothelial cell

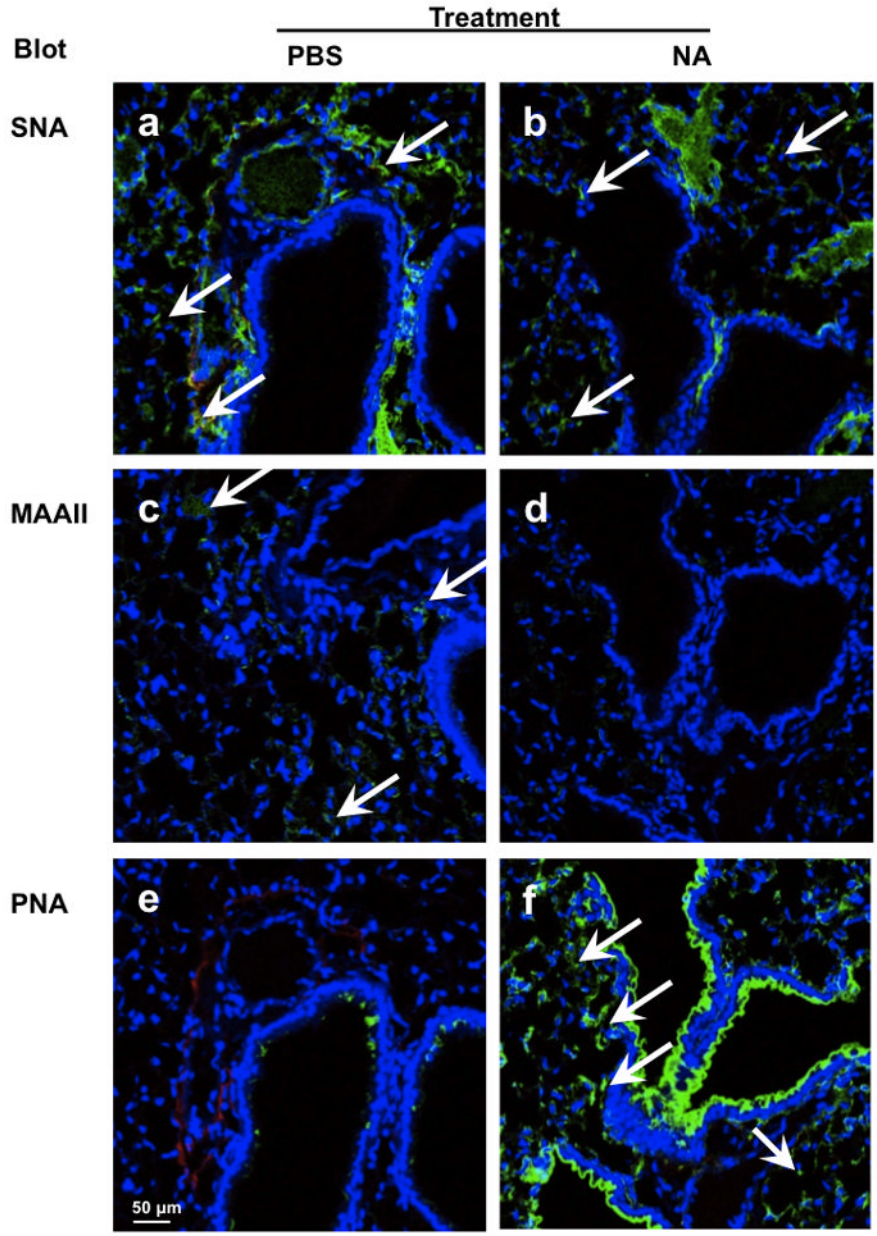

Figure 1. Intratracheal instillation of NA desialylates mouse lung tissue

PBS (a, c, e) or NA (b, d, f) was administered i.t. into the lungs of CD1 outbred mice. After 30 min, the lungs were fixed, paraffin-embedded, and processed for probing with biotinylated SNA (a, b), MAAII (c, d), or PNA (e, f) lectins followed by Cy2-conjugated streptavidin (green) and counterstained with DAPI (blue). Magnification 60X, arrows indicate positive lectin staining in alveolar area. Each photomicrograph is representative of 3 independent experiments. Bar in panel e, lower left, represents 50 μm.

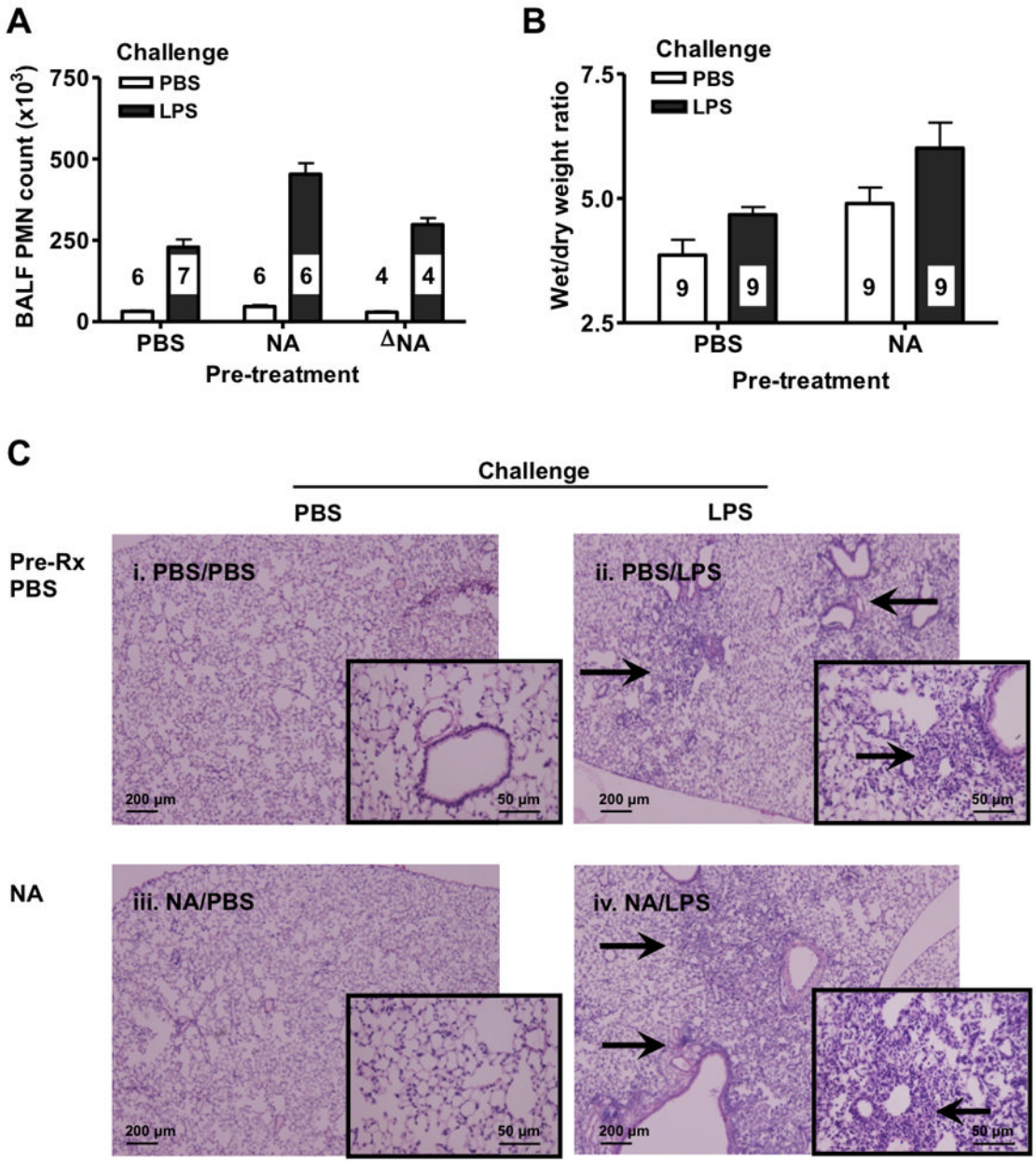

Figure 2. Prior desialylation potentiates LPS-induced ALI

CD1 outbred mice were administered PBS, NA, or heat-inactivated NA (ΔNA) i.t., followed 30 min later by i.t. challenge with PBS or LPS. (A) The PMN number in BALF was determined after 18 h. Each vertical bar represents mean (+/-SEM) BALF cell counts. The n for each group is indicated in each bar. PBS/LPS vs. PBS/PBS, $p<0.0001$; NA/PBS vs. PBS/PBS, $p>0.5$; NA/LPS vs. PBS/LPS, $p<0.0001$. (B) The wet-to-dry weights of treated mouse lungs were determined after 18 h and the wet/dry weight ratios were calculated. The n for each group is indicated in each bar. Each vertical bar represents mean (+/- SEM) lung wet/dry weight ratio. Both the LPS ($p=0.009$) and NA effects ($p=0.002$) were independently significant. The effects of NA and LPS appeared to be additive. (C) Lung tissue from each group was collected after 18 h and processed for H&E staining. Magnification 40X, with insert (200X) emphasizing the interstitial area. Arrows indicate PMN enriched area. Each photomicrograph is representative of 3 independent experiments.

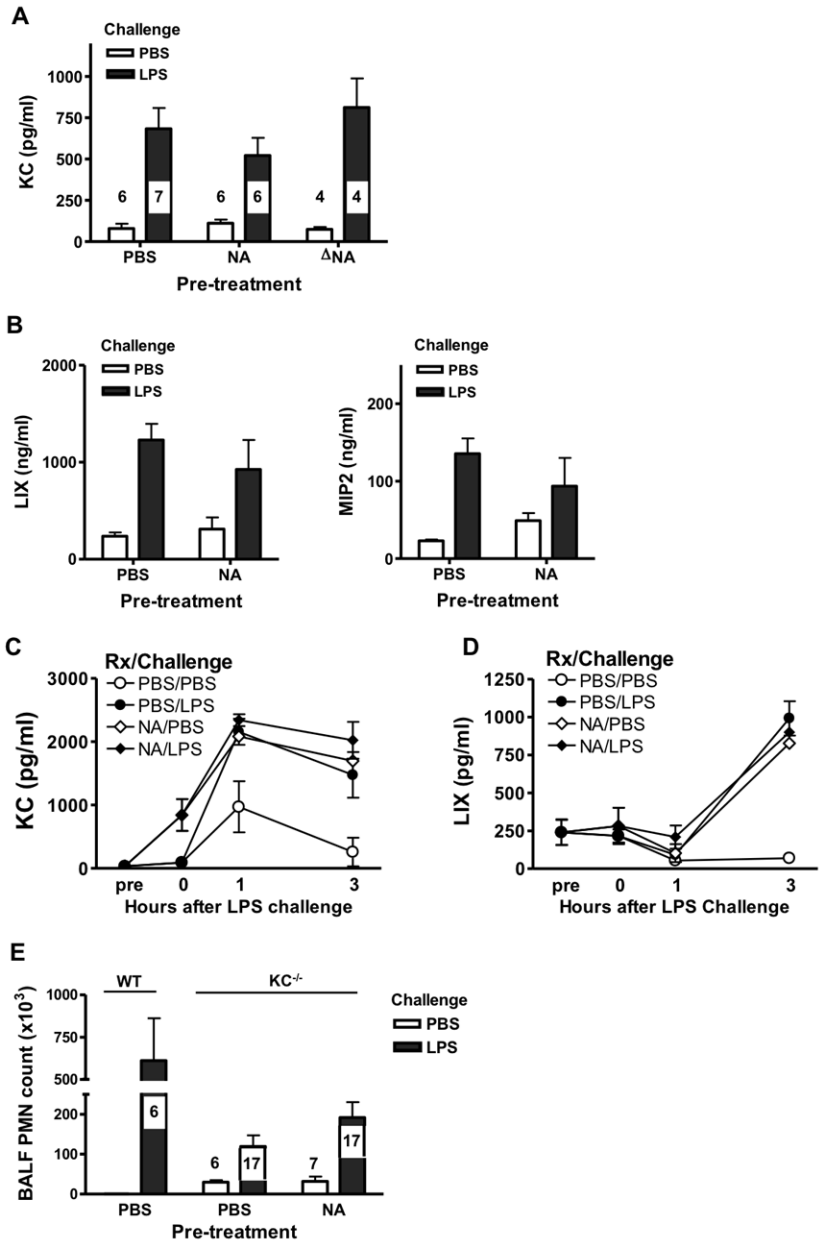

Figure 3. Prior desialylation does not alter LPS-induced chemokine production

CD1 outbred mice were treated i.t. with PBS, NA, or heat-inactivated NA (ΔNA), followed 30 min later by i.t. challenge with LPS or PBS. (A) After 18 h, the KC concentration in BALF was determined. The n for each group is indicated in each bar. PBS/LPS vs. PBS/PBS; NA/LPS vs NA/PBS; ΔNA/LPS vs. ΔNA/PBS each $p<0.0001$. NA, either with or without LPS challenge had no effect (B) The LIX and MIP2 concentrations in BALF were determined. A representative experiment from two independent studies with 3 mice in each group is shown. The results in panel B are similar to panel A. (C and D). The KC (C) or LIX (D) concentration in BALF at specific time points was determined. Each symbol represents mean (+/-SEM) concentration in pg/ml. Data are pooled from 4 mice of 2 independent experiments. C. At 3 h NA/LPS vs. PBS/PBS, $p<0.05$. At neither 1 h nor 3 h were treatments significantly different from each other by the Tukey multiple comparisons procedure. D. At 3 hr NA/PBS, PBS/LPS and NA/LPS treatments all similar, and were

increased vs PBS/PBS, $p<0.01$. (E) KC knockout ($KC^{-/-}$) or wild-type (C57BL/6) mice were treated i.t. with PBS, NA, or ΔNA followed 30 min later by i.t. challenge with PBS or LPS. The PMN number in BALF was determined after 18 h. The n for each group is indicated in each bar. PBS/LPS in $KC^{-/-}$ mice vs. PBS/LPS in wild-type C57BL/6 mice, $p=0.014$. In $KC^{-/-}$ mice NA/LPS vs. PBS/LPS and NA/PBS, $p<0.05$ by Tukey procedure.

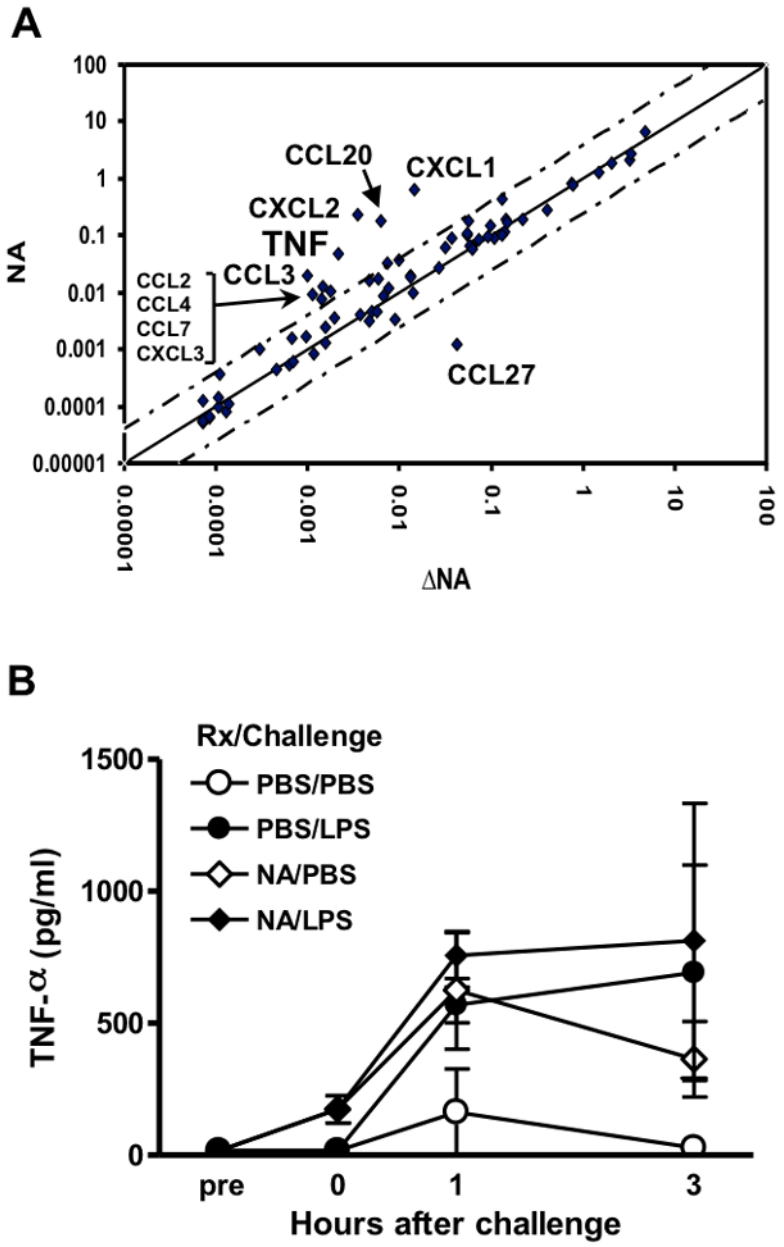

Figure 4. Desialylation alters lung gene expression

(A) CD1 outbred mice were treated i.t. with heat-activated NA (ΔNA) or NA, and the gene expression in lung tissue was determined at 30 min. (B) Mice were pretreated with PBS or NA, followed 30 min later by i.t. challenge with PBS or LPS. The TNF-α concentrations in the BALF at the indicated time points were determined. Data are pooled from 2 independent experiments with a total of 4 mice per group at t=0 and 3h, and 2 mice per group at t=1h. At 1 h and 3 h after LPS challenge, none of the differences in TNF-α production was statistically significant.

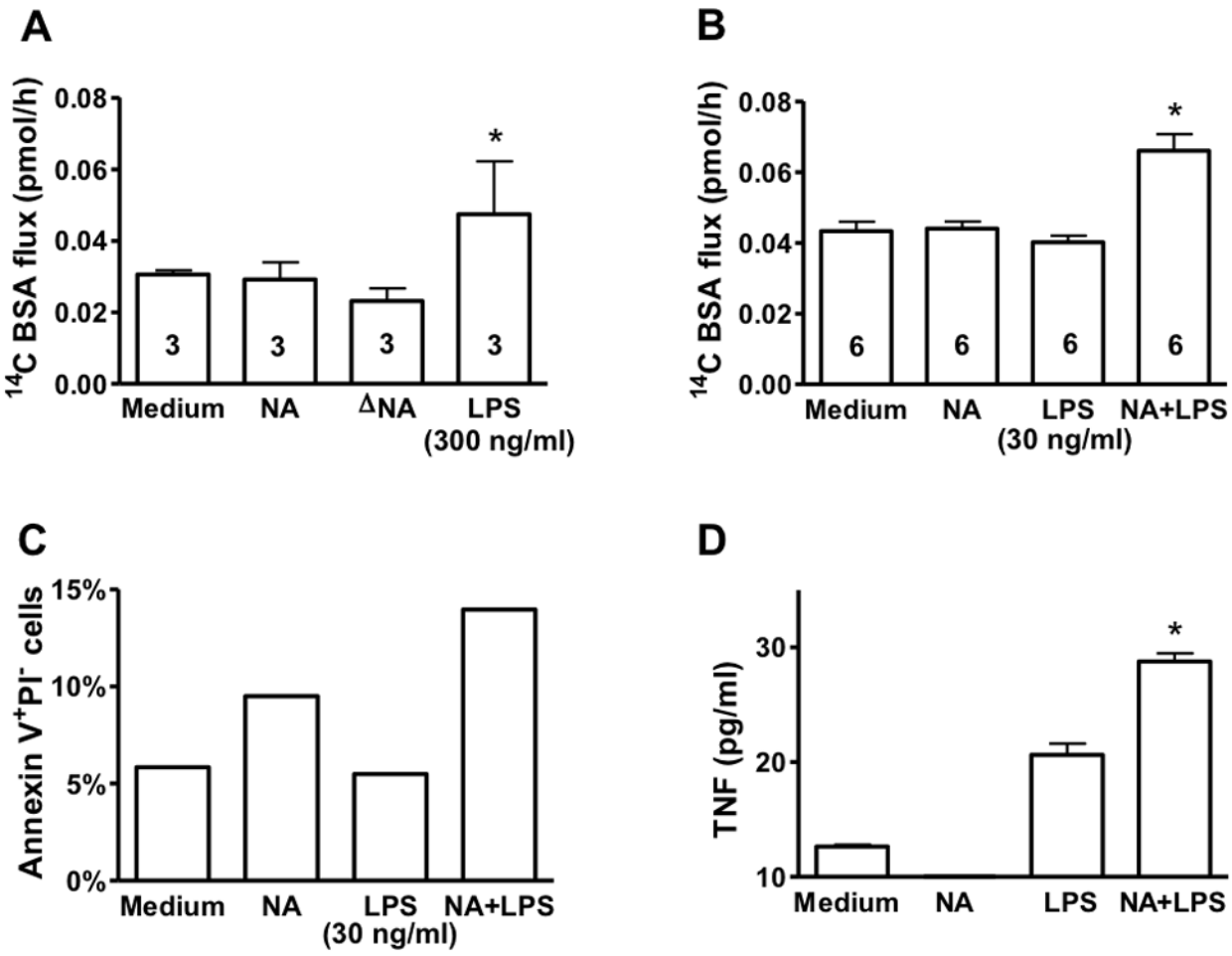

Figure 5. Desialylation sensitizes endothelial cells to LPS-induced barrier disruption

(A) Post-confluent HMVEC-L monolayers were treated for 6 h with medium alone, NA (30 mU/ml), heat-inactivated NA (ΔNA), or LPS (300 ng/ml). Transendothelial ^{14}C-BSA flux in pmol/h immediately after 6 h was determined. The n for each group is indicated in each bar. LPS, but not NA treatment, increased BSA flux (*$p<0.05$ compared to each of the other treatments by the Tukey multiple comparisons procedure). (B) Post-confluent HMVEC-L monolayers were treated with medium alone, NA (30 mU/ml), LPS (30 ng/ml), or both NA and LPS (NA+LPS) and transendothelial ^{14}C-BSA flux immediately after 6 h was determined. *NA + LPS vs. all other treatments, $p< 0.001$ by the Tukey procedure. (C) Post-confluent HMVEC-L monolayers were treated with medium alone, NA (30 mU/ml), LPS (30 ng/ml), or both NA and LPS (NA+LPS) for 6 h, suspended and stained with Annexin V and PI for flow cytometry analysis. Mean (+/- SEM) percentage of cells undergoing apoptosis (Annexin V$^+$ PI$^-$) for each group was shown. (D) TNF-α production (mean +/- SEM) in culture supernatants from C was determined. LPS vs. medium, $p<0.01$; *NA+LPS vs. LPS, $p<0.01$; NA vs. medium=NS.

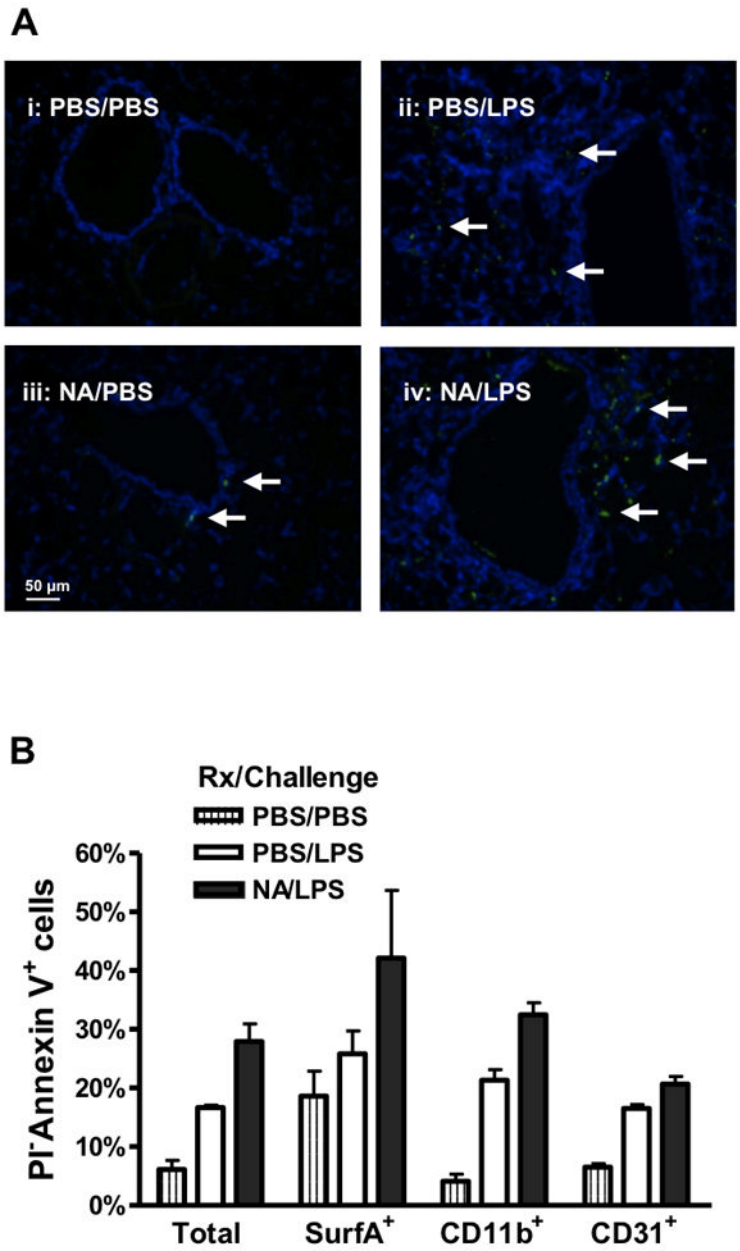

Figure 6. Desialylation prior to LPS challenge enhances lung and immune cell apoptosis

CD1 outbred mice were pretreated with PBS or NA before i.t. challenge with LPS or PBS. (A) After 18 h lung tissues were fixed, processed for TUNEL staining (green) and counterstaining with DAPI (blue). Each photomicrograph is representative of 3 independent experiments. Magnification: 60X. Arrows indicate apoptotic cells. (B) After 18 h, single cell suspensions were prepared from the lungs of challenged mice using collagenase and DNAse I digestion, and stained with Surfactant A-, CD11b- or CD31- specific antibodies followed by Annexin V and PI staining for flow cytometric analysis. Each vertical bar represents the percentage of $PI^-Annexin\ V^+$ cells (+/- SEM). Data are composite of four separate experiments in which groups of 5 mice for each treatment were pooled, stained and analyzed in each experiment. PBS/LPS vs. PBS/PBS, $p<0.05$;. NA/LPS vs. PBS/LPS, $p<0.01$. Among the three cell types, the difference between NA/LPS vs. PBS/LPS was statistically significant only for $CD11b^+$.

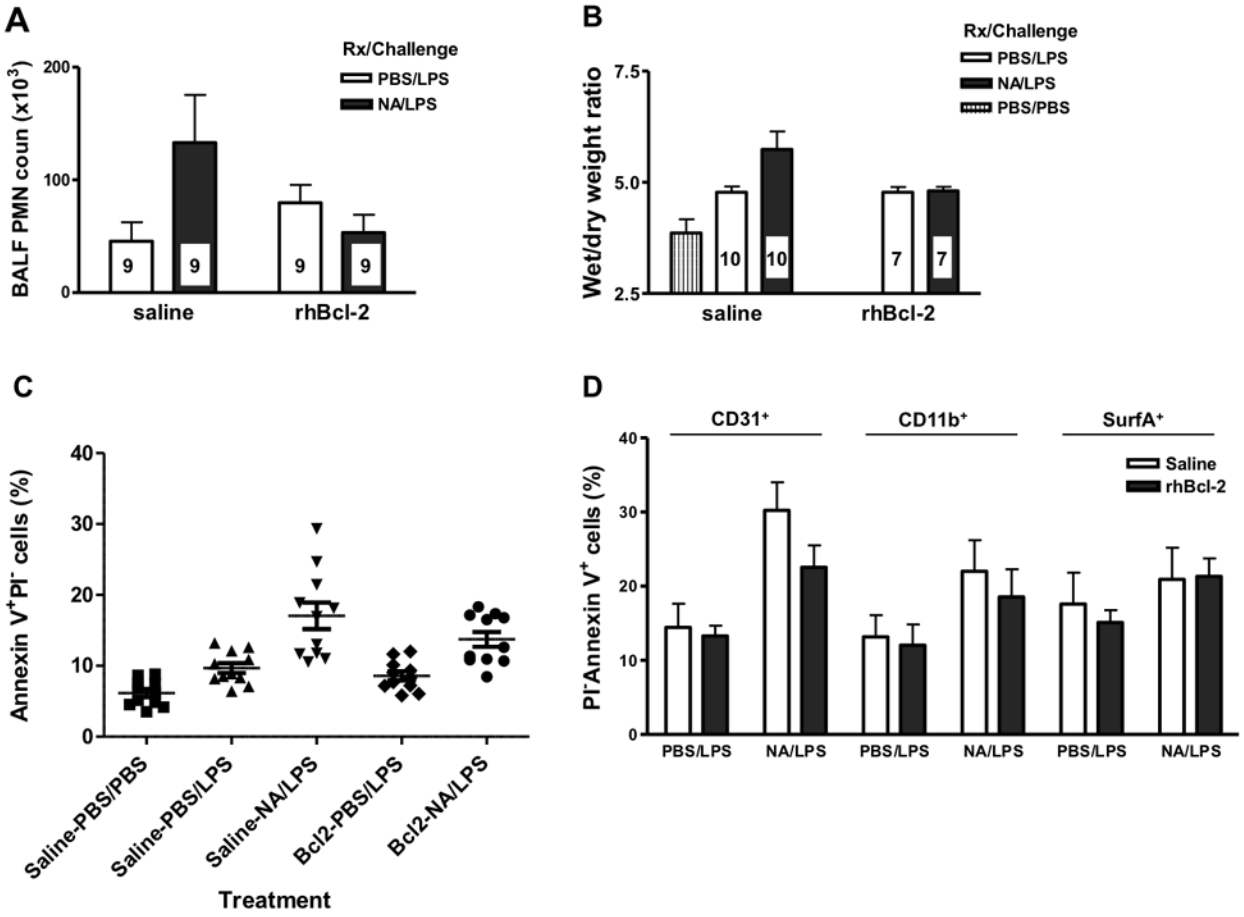

Figure 7. Bcl-2 inhibits NA-potentiated apoptosis

(A) CD1 outbred mice were injected i.p. with saline vehicle or rhBcl-2 (1 μg) in saline for 30 min, then PBS or NA i.t., followed 30 min later by i.t. challenge with LPS. The PMN number in BALF was determined after 18 h. Each vertical bar represents mean (+/-SE) BALF cell counts. Saline/ PBS/LPS vs. rhBcl-2/PBS/LPS =NS. Saline/NA/LPS vs. saline/ PBS/ LPS, $p<0.05$ by Tukey test. rhBcl-2/NA/LPS vs. rhBcl-2/PBS/LPS=NS.

(B) The wet and dry weights of treated mouse lungs were determined after 18 h and the wet/ dry weight ratios were calculated. Each vertical bar represents mean (+/- SEM) lung wet/dry weight ratio. The n for each group is indicated in each bar. Saline/NA/LPS vs. saline/PBS/ LPS, $p<0.05$ by Tukey test; rhBcl-2/NA/LPS vs. rhBcl-2/PBS/LPS=NS. (C) After 18 h, single cell suspensions were prepared from 5 lungs of treated mice in each group and analyzed as in Figure 6. Each point on the scatter plot represents the percentage of PI^-Annexin V^+ cells from at least triplicate measurements in 3 independent experiments in which each of the lungs from 5 mice were pooled. Saline/NA/LPS vs. saline/PBS/LPS ($p<0.001$) and rhBcl-2/NA/LPS vs. rhBcl-2/PBS/LPS ($p<0.05$). Saline/NA/LPS vs. rhBcl-2/ NA/LPS=NS. (D) Single cell suspensions were stained with CD31 for endothelial cells, CD11b for myeloid cells, and Surfactant A for epithelial cells before Annexin V-PI staining. Each vertical bar represents the percentage of PI^-Annexin V^+ cells. Data are combined from 4 independent experiments in which each of the lungs from 5 individual mice were pooled for each variable in each experiment (i.e. total of 20 mice pooled). With prior saline treatment, the number of apoptotic cells increased in all populations with NA treatment ($p<0.0001$ for $CD11b^+$, $p=0.0002$ for $CD31^+$, $p=0.077$ for $SurfA^+$). Bcl-2 pre-treatment

decreased the number of apoptotic cells in the $CD11b^+$ ($p=0.032$) population but not for the $CD31^+$ ($p=0.063$) and $SurfA^+$ populations ($p>0.50$).